

An Experimental Model of Non-rafting Collisions Between Ice Floes Caused by Monochromatic Water Waves

L. G. Bennetts¹, L. J. Yiew¹, M. H. Meylan², B. J. French³ and G. A. Thomas³

¹School of Mathematical Sciences, University of Adelaide, South Australia 5005, Australia

²School of Mathematical and Physical Sciences, University of Newcastle, Callaghan NSW 2308, Australia

³National Centre for Maritime Engineering and Hydrodynamics, Australian Maritime College, Launceston 7250, Australia

Abstract

An experimental model of wave-induced collisions between two sea-ice floes is presented. The model was implemented in a laboratory wave basin. Monochromatic incident waves were used, with frequencies between 0.5 Hz and 1.5 Hz, and wave heights 20 mm and 40 mm. An algorithm is proposed to identify collisions and collision velocities from recorded floe motions. Collisions are shown to be strongest and most frequent for mid-range frequencies and the larger wave height.

Introduction

Discrete chunks of floating sea ice (ice floes) partially cover a vast region of the ocean surface, up to hundreds of kilometres in width. The region is the interface between the open ocean and the fully ice-covered ocean. The floes are on the order of tens to hundreds of metres in diameter and centimetres to metres in thickness. The region is highly dynamic, due to the presence of ocean surface waves. Waves either propagate into the region from the open ocean or are generated by local fetch.

Waves set the floes in motion. In particular, they induce lateral motions, consisting of an oscillatory (surge) component and a drift component (Shen & Ackley [9]; Meylan et al. [7]). Lateral motions cause floes to collide with one another (Martin & Becker [4]) if drift velocities of adjacent floes differ sufficiently, or surge motions are sufficiently large (with respect to floe separations) and sufficiently out of phase. Collisions (i) dissipate wave energy, and hence limit the distance waves propagate, and (ii) cause floes to erode and break into rubble at their edges (McKenna & Croker [6]). The strength and frequency of collisions determines the proportion of wave energy attenuated and the extent of erosion/breaking. Further, if the relative pitch of the colliding floes is sufficiently out of plane, the floes can raft (Bennetts & Williams [1]). Rafting is a key agent of ice thickness growth (Dai et al. [2]). It also produces new areas of open water for ice production.

Wave-induced collisions between floes, hence, impact the dynamic and thermodynamic properties of the ice cover (Shen et al. [10]; Martin & Becker [5]). However, relatively few models of wave-induced collisions have been developed. Mathematical models were developed in the early 1990s (McKenna & Croker [6]; Shen & Ackley [9]; Rottier [8]; Gao [3]). The models are not yet sufficiently robust to be integrated into large-scale coupled models. For example, the models are based on the assumption that floes do not influence the surrounding wave field, which is valid for large wavelength-to-floe-diameter ratios only.

An experimental model of collisions between two floes is presented here. The model was implemented in a wave basin. A mechanical wave maker was used to generate monochromatic incident waves and induce floe collisions. A range of different incident wave frequencies and two incident wave heights were tested. Edge barriers were attached to the model floes to restrict

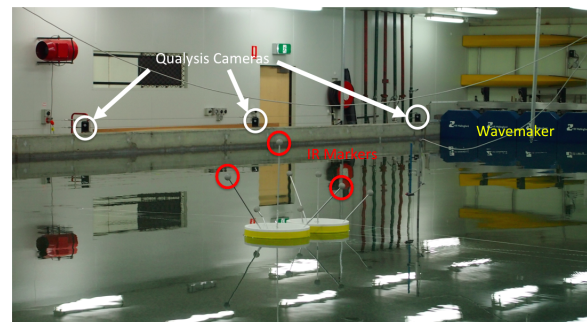


Figure 1. Photo of experimental set-up.

rafting events, and hence investigate collisions only.

A non-intrusive tracking system measured floe motions during the tests. An algorithm is proposed here to identify collisions from the floe motions. Collision velocities are also calculated. Analysis of the collision data indicate collisions are strongest and most frequent for mid-range wave frequencies and the larger wave height.

Experimental Model

An experimental model of wave-induced collisions of two identical floes was implemented in the model test basin (MTB) of the Australian Maritime College, Launceston. The MTB is 35 m long and 12 m wide. The ambient fluid depth was 800 mm.

The floes were modelled by thin Nycel plastic disks. (Nycel is a closed-cell expanded foam rigid polyvinyl chloride sheet with a thin plastic coating.) The disks were of $D = 400$ mm diameter, 15 mm thickness and 1.68 kg mass. At a geometric scale of 1:100, this models ice floes of 40 m diameter, 1.5 m thickness and 1.73×10^6 kg mass.

A mechanical wave maker was used to generate regular (monochromatic) waves. Wave heights 20 mm and 40 mm, and frequencies between 0.5 Hz and 1.5 Hz were tested. The corresponding wavelengths were approximately 0.69 m to 4.85 m. The corresponding steepnesses, which are equivalent to full scale steepnesses, were approximately 0.4 % to 5.8 %. Figure 1 shows a photo of the experimental set-up, including a portion of the wave maker. A static beach was located at the opposite end of the MTB to the wave maker, in order to reduce the waves reflected at this boundary.

The floes were located one behind the other, in line with the direction of the incident waves. The floe closest to the wave maker is referred to as the front floe, and the floe farthest from the wave maker is referred to as the rear floe. In equilibrium, the closest points of the floes were separated by 20 mm. Figure 2 shows a schematic plan view of the MTB, including the equilibrium floe locations.

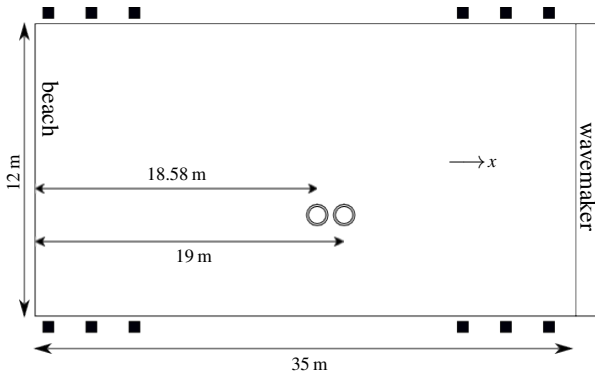


Figure 2. Schematic plan view of MTB for tests. Concentric circles denote floes. Black squares indicate locations of cameras used by Qualysis system.

Polystyrene edge barriers were attached to the floes. The barriers were 50 mm high and 25 mm thick. They were used, primarily, to restrict the floes from rafting. They also (slightly) modify the individual response of the floes to wave motion, e.g. surge and drift, by preventing waves overwashing the floes and increasing the surface area of the floe edges.

The floes were moored to the sides of the MTB using fishing line. The mooring restricted the floes to move only a certain distance up or down the MTB. It therefore allowed for multiple collisions in a single test, and returned the floes to their initial configuration at the start of each new test. The influence of the mooring on the results is discussed in the next section.

Four spherical polystyrene, infrared (IR) markers, with 30 mm diameters, mounted on light-weight aluminium cylinders, were attached to each floe. Three IR markers on the rear floe are labelled in figure 2. The markers and mounts were sufficiently light to have negligible influence on floe motions.

The location of the markers was measured stereoscopically by the Qualysis motion tracking system, via a set of IR cameras. Three cameras are labelled in figure 1. Figure 2 indicates the locations of the cameras.

Analysis

Collision Detecting Algorithm

Translational motions in the direction opposite to that of the incident waves, i.e. up the MTB, are used to detect collisions. A coordinate, x , is assigned to the motion in this direction (as indicated on figure 2). The front floe is assigned an x -coordinate, x_f , with origin at its centre. Similarly, the rear floe is assigned an x -coordinate, x_r , with origin its centre.

The Qualysis system provides time series $x_f(t_n)$ and $x_r(t_n)$ for motions of the front and rear floes in the x -direction. The motions are at times $t_n = n/200$ s ($n = 1, \dots, 10248$), i.e. 200 Hz capture frequency from 60.24 s records.

For each test, the following algorithm, based on the separation of the two floes, is applied to detect collisions.

- 1a. Calculate the separation $|x_f - \hat{x}_r|$, where $\hat{x}_r = x_r - D$.
- 1b. Provisionally identify times at which separations are less than the tolerance 1 mm, as collision times.

The algorithm does not account for small changes to the separations due to rotational, pitch motions of the floes.

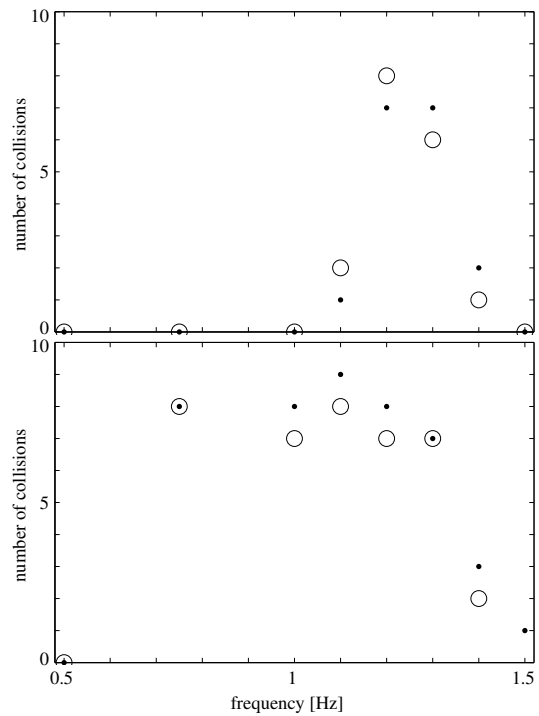


Figure 3. Number of collisions per test, as a function of incident wave frequency. Incident wave height 20 mm (top panel) and 40 mm (bottom). Bullets and circles distinguish repeated tests.

The 200 Hz resolution does not reliably capture separations less than 1 mm during sharp, energetic collisions. Therefore, the following algorithm, based on excitation of high frequencies by sharp collisions, is also applied to detect collisions.

- 2a. Provisionally identify times at which separations are less than the tolerance 5 mm, as collision times.
- 2b. Apply a third-order Butterworth filter to extract the high-frequency components of the signals.
- 2c. Retain the provisional collision times if the high-frequency signals of both the front and rear floes are greater than the threshold 0.5 mm at those times.

The three final steps, below, are applied to the overall algorithm to eliminate repeated collisions.

3. Merge provisional collision times provided by the separation and high-pass-filter algorithms.
4. Assign an interval of radius 2 s around each collision time. Merge overlapping intervals, and identify the resulting interval as containing a single collision.
5. Identify the time at which the minimum separation occurs in the interval as the collision time.

Results

Figure 3 shows the number of collisions per test, as a function of incident wave frequency. Results are separated according to incident wave height, 20 mm or 40 mm. Most tests were repeated. In all cases, the number of collisions recorded in the repeated tests differed from the original tests by at most one.

For a 20 mm incident wave height, collisions only occurred for incident wave frequencies between 1.1 Hz to 1.4 Hz. Incident

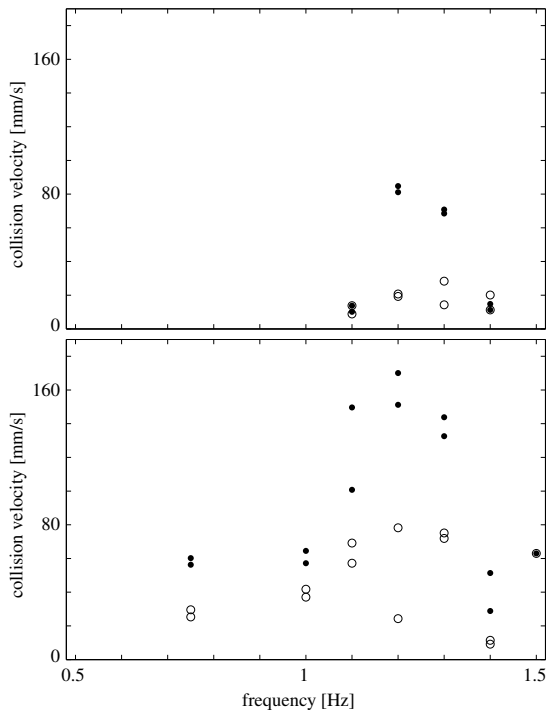


Figure 4. Collision velocity, as a function of incident wave frequency. Incident wave height 20 mm (top panel) and 40 mm (bottom). Bullets denote mean collision velocity during test. Circles denote velocity of first collision in test.

frequencies 1.2 Hz and 1.3 Hz caused the largest number of collisions, six to eight. Incident frequencies 1.1 Hz and 1.4 Hz only caused one to two collisions.

For a 40 mm incident wave height, collisions occurred in all tests except the lowest incident wave frequency, 0.5 Hz. Seven to nine collisions occurred in the tests with incident wave frequencies between 0.75 Hz and 1.3 Hz. For the two highest incident wave frequencies, 1.4 Hz and 1.5 Hz, far fewer collisions occurred, only one to three.

Figure 4 shows collision velocity, as a function of incident wave frequency, and separated according to incident wave height. Collision velocity is calculated as the mean of the velocity of the front floe in the negative x -direction prior to a collision and the rear floe in the positive x -direction prior to a collision, i.e. velocities towards one another. Floe velocities are calculated as the slope of a linear regression to the time series of motions in the x -direction, over 10 time steps prior to a collision.

Figure 4 shows both the mean collision velocity per test and the velocity of the initial collision in each test. The initial velocity is far smaller than the mean velocity. Following the initial collisions, the strength of collisions are augmented by the mooring. This is discussed further below.

Both the mean velocity and the initial velocity share the same qualitative behaviours as the corresponding number of collisions shown in figure 3. The collision velocity is small when a small number of collisions occur during a test, and large when a large number of collisions occur during a test. However, for the 40 mm incident wave height, the collision velocity shows a strong peak for incident frequencies 1.2 Hz to 1.3 Hz, which contrasts with the weak peak shown by the number of collisions.

Figure 5 shows examples of the floe motions in the 20 mm incident wave height tests. The examples illustrate the regime changes indicated by the top panels of figures 3 and 4. For the

lowest incident frequency, 0.5 Hz, surge dominate the floe motions. The floes do not collide because they surge in phase with one another.

Surge motions of the two floes become increasingly out of phase as incident frequency increases. Simultaneously, wave scattering becomes stronger and surge amplitudes decrease (Meylan et al. [7]). The incident wave also begins to make the floes drift. A combination of these effects forces floe collisions.

The incident frequency 1.1 Hz marks the onset of collisions. The initial collision forces the floes apart, only to be pulled back towards one another by the mooring. (The influence of the mooring is visible in low frequency oscillations of the floes.) However, wave forces between the two floes prevent further collisions.

The incident frequency 1.2 Hz causes the maximum number of collisions, and the strongest collisions. Here, collisions are strong enough to excite a mooring force that overcomes the wave forces between the floes. Hence, after transient motions in which collision strength increases, the floes collide at regular intervals determined by the period of the mooring force, and with consistent strength.

A 1.5 Hz incident frequency does not generate surge amplitudes large enough to cause collisions. Instead, scattered waves between the floes force the floes apart. The force of the scattered waves is not strong enough to strongly excite the mooring forces. A steady situation is developed, in which the forces of the scattered waves and the mooring are balanced.

Figure 6 shows example floe motions that illustrate the regime changes with incident wave frequency for a 40 mm incident wave height. For the lowest incident frequency, 0.5 Hz, again the floes surge in phase with one another, and hence do not collide. An incident frequency of 0.75 Hz marks the onset of collisions for the larger incident wave height. The onset frequency here is far lower than that of the 20 mm incident wave height tests, which indicates collisions are a highly nonlinear phenomenon.

The larger wave height also produces stronger collisions. Thus the regular collisional structure, dictated by the mooring, governs a far larger spectrum of incident frequencies. The regime includes the incident frequencies 0.75 Hz and 1.1 Hz shown in figure 6. For the 1.1 Hz incident frequency, collision strength increases over the recorded time interval, and does not settle by the end of the interval.

For the highest incident frequency, 1.5 Hz, the 40 mm incident wave height, unlike the 20 mm height, produces surge amplitudes that trigger an initial collision. However, subsequent motions are qualitatively identical to those produced by the smaller incident wave height. The motions settle to a situation in which scattered wave forces and mooring forces balance one another. No further collisions occur.

Summary and Discussion

An experimental model of wave-induced collisions between two sea-ice floes has been presented. The model was implemented in the model test basin of the Australian Maritime College. An algorithm was proposed to identify collisions and collision velocities from recorded floe motions. Collisions were shown to be strongest and most frequent for mid-range frequencies and the larger wave height tested.

The experiments are essentially fundamental research. The experiments do not model wave-induced ice floe collisions in the ocean for the following reasons.

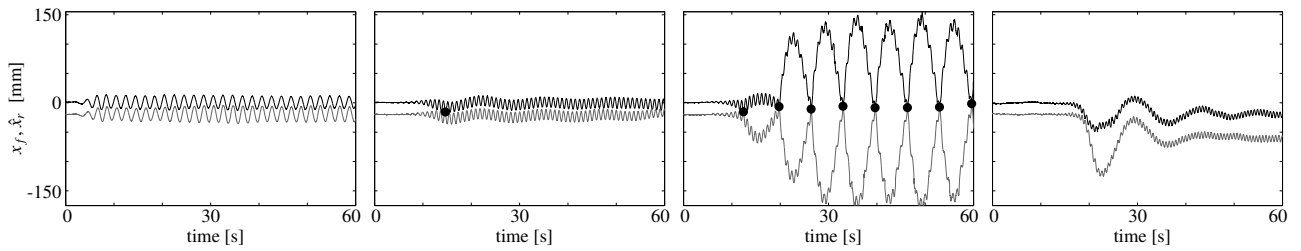


Figure 5. Example motions in x -direction of front floe (x_f , black curve) and rear floe (\hat{x}_r , grey) during tests with incident wave height 20 mm. Incident wave frequency 0.5 Hz (left-hand panel) 1.1 Hz (middle-left), 1.2 Hz (middle-right) and 1.5 Hz (right). Bullets denote collisions.

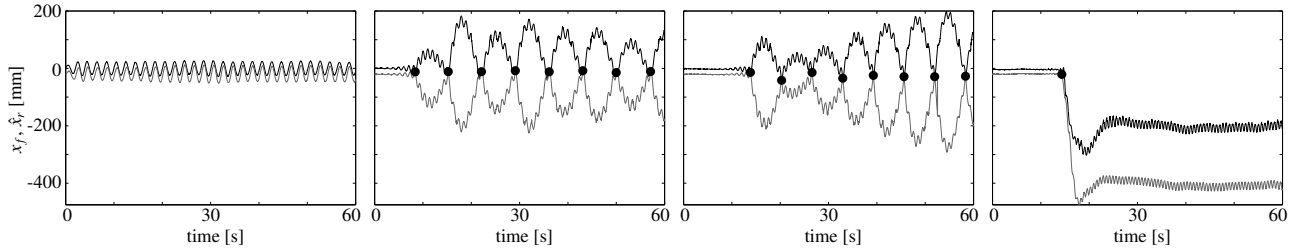


Figure 6. As in figure 5 for incident wave height 40 mm. Incident wave frequency 0.5 Hz (left-hand panel), 0.75 Hz (middle-left), 1.1 Hz (middle-right) and 1.5 Hz (right).

- i. Monochromatic incident waves were used, whereas ocean waves are composed of a spectrum of waves of different frequencies and directions.
- ii. Collisions between two identical floes were modelled, whereas collisions in the ice-covered ocean involve a large number of floes of different shapes and sizes.
- iii. Moorings were used to restrain the model floes, whereas, in the ocean, ice floes are restrained by surrounding floes. Although mooring forces superficially resemble the ricochet effect of a floe colliding with surrounding floes, the regularity of the mooring force is highly unlikely to model collisions with surrounding floes.

However, the model provides the following insights on wave-induced collisions between ice floes.

- i. The onset of collisions, and their subsequent strength and frequency, are highly nonlinear with respect to incident wave height.
- ii. Both the phase and the amplitude of surge motions determine the onset of collisions.
- iii. Wave forces between floes affect the strength and frequency of collisions for high frequency incident waves.

These insights will assist development of mathematical/numerical collision models.

Acknowledgements

The experiments were funded by the Australian Maritime College. LGB acknowledges funding support from the Australian Research Council (DE130101571) and the Australian Antarctic Science Grant Program (Project 4123). MHM acknowledges support of the Office of Naval Research. LJY holds a PhD scholarship funded by the Australian Research Council.

References

- [1] Bennetts, L. G. and Williams, T. D., Water wave transmission by an array of floating disks, *ArXiv*, 1403.3766.
- [2] Dai, M., Shen, H. H., Hopkins, M. A. and Ackley, S. F., Wave rafting and the equilibrium pancake ice cover thickness, *J. Geophys. Res.*, **109**, 2004, C07023.
- [3] Gao, L., *Ice floe collisions under wave action in the marginal ice zone*, Master's thesis, Memorial University of Newfoundland, St. Johns, 1992.
- [4] Martin, S. and Becker, P., High-frequency ice floe collisions in the Greenland Sea during the 1984 marginal ice zone experiment, *J. Geophys. Res.*, **92**, 1987, 7071–7084.
- [5] Martin, S. and Becker, P., Ice floe collisions and their relation to ice deformation in the Bering Sea during February 1983, *J. Geophys. Res.*, **93**, 1988, 1303–1305.
- [6] McKenna, R. F. and Croker, G. B., Wave energy and floe collisions in marginal ice zones, in *Ice Technology for Polar Regions, proceedings of the 2nd International Conference on Ice Technology*, ed. T. Murphy, Computational Mechanics Publications, Southampton, 1990, 33–41.
- [7] Meylan, M. H., Yiew, L. J., Bennetts, L. G., French, B. J. and Thomas, G. T., Surge motion of an ice floe in waves: comparison of theoretical and experimental models, *Annals Glaciol.*, **56**, 2014, In Press.
- [8] Rottier, P. J., Floe pair interaction event rates in the marginal ice zone, *J. Geophys. Res.*, **97**, 1992, 9391–9400.
- [9] Shen, H. H. and Ackley, S. F., A one-dimensional model for wave-induced ice-floe collisions, *Annals Glaciol.*, **15**, 1991, 87–95.
- [10] Shen, H. H., Hibler, W. D. and Lepparanta, M., The role of floe collisions in sea ice rheology, *J. Geophys. Res.*, **92**, 1987, 7085–7096.